Entropy Sources in Equilibrium Conditions over a Tropical Ocean

CHARLES WARNER

Hindhead, Surrey, United Kingdom

(Manuscript received 28 April 2003, in final form 10 February 2004)

ABSTRACT

Confusion has existed as to sources of entropy due to irreversible processes in the atmosphere, the total of which matches the export of entropy by radiation. What is the mechanical efficiency of convection? For an ideal tropical oceanic system in radiative–convective equilibrium, relative magnitudes of sources of entropy are reviewed—from both observations and numerical model results. Recycling of moisture is shown to be important. Leading terms are those relating to evaporation of precipitation, water loading by falling precipitation, and mixing of unsaturated parcels of air, contributing roughly 37%, 30%, and 15% of the total irreversible production of entropy, respectively. Evaporation from the surface accounts for 11%. The remaining 7% is due to turbulent kinetic energy, generation of gravity waves, and sensible heating at the surface.

A mechanical efficiency of conversion of heat supply at the surface into kinetic energy of the direct circulation, ≈2.0%, is obtained after the budget study. The leading contribution to the conversion is due to the effect of hydrometeors. Drag of hydrometeors is split into two components based on relative contributions of form drag plus water loading (50%) and frictional drag (50%); however, only the former contributes to the direct circulation. The contribution of turbulent kinetic energy is found to be small.

Results from the budget study are found to correspond with the finding of a threshold in values of convective available potential energy by Roff and Yano, and with numerical results from a three-dimensional model of convective equilibrium by Shutts and Gray.

1. Introduction

a. Background

In a tropical oceanic context, the operation of cumulus convection as a heat engine has been discussed. Work by Rennó and Ingersoll (1996, hereafter RI) and Emanuel and Bister (1996, hereafter EB) was on the basis that most of the convective available potential energy (CAPE) of tropical convection goes into generation of kinetic energy. Later Rennó (2001) explained that heat engine theory can be considered satisfactory if an appropriate efficiency of conversion from potential to kinetic energy can be determined. Recently Goody (2003) has provided insights from a very simple treatment.

To determine the mechanical efficiency of convection, it is necessary to evaluate all of the irreversible sources of entropy involved in the convection. A tropical oceanic system in radiative–convective equilibrium is considered. In the location of the ascending branch of the circulation, it is assumed that CAPE is sufficient to yield deep convection. Energy and entropy budgets have been compiled incompletely by several authors, notably EB, Goody (2000), and Pauluis and Held (2002, hereafter PH). Here some confusing issues are clarified, and a unified picture is presented. After determination of the budget of entropy production, the terms of kinetic energy dissipation are summed to obtain an efficiency of heating conversion at the surface into kinetic energy. Results are related to other findings.

b. Fractional area coverage by updrafts and rate of precipitation

Important in this work is an assessment of the fractional area coverage σ by deep convective updrafts. A representative value for the whole troposphere for conditions of radiative–convective equilibrium is sought. Warner (1984a)[1] and Warner and Grumm (1984) were particularly concerned to assess from observations the fractional area coverage σ in a well-observed Bay of Bengal monsoon depression, because at the time it was thought that ascent could satisfactorily be treated as a

Corresponding author address: Dr. Charles Warner, 10 Thirlestane Court, Tilford Road, Hindhead, Surrey, GU26 6SH, United Kingdom.
E-mail: jetsamoocow@clara.co.uk

[1] The updated values for centripetal acceleration and the Coriolis acceleration are $\sim 1.7 \times 10^{-3}$ and 0.9×10^{-3} m s^{-2}, respectively, p. 144.

© 2005 American Meteorological Society

Unauthenticated | Downloaded 10/23/21 01:08 AM UTC

large-scale phenomenon, in contrast to the previous emphasis on "hot towers" by Riehl and Simpson (1979). Studies of this depression were reviewed by Johnson and Houze (1987). Warner and Grumm used several different approaches. Warner (1984a) found $\sigma = 1\%$ by radar echoes commensurate with a rainfall rate of 6 mm h^{-1}, in an area in which the average rainfall was about 1 cm day^{-1}. Intense radar echoes signify present or recent updrafts, so this finding is probably representative of deep updrafts. It is found appropriate below to assume an average rainfall of 4.9 mm day^{-1}, so Warner's $\sigma = 1\%$ should be referred to an area of double the size, giving $\sigma = 0.5\%$. Warner and Grumm (1984) studied encounters of aircraft with updrafts on traverses through the depression. Findings displayed in their Table 1 show a variety of values, mostly not far from 0.5%. Knowledge was gained of sizes and velocities of cumulus clouds by photogrammetry, and their overall properties were assessed by counts of clouds in various size categories over various domains. For individual cumulus clouds σ was on the order of tenths of 1%. There were great uncertainties due both to difficulties of measurement, and to the sporadic nature of convection, developing over time and varying in space. The studies by Warner and Grumm of this depression suggest that $\sigma \approx 0.5\%$.

Warner (1981) made assessments of σ for the case of 10 December 1978 during the Winter Monsoon Experiment. In terms of cumulonimbus clouds, nine were counted in an area of 25 000 km^2, and this led to an estimate of $\sigma \approx 0.1\%$, based upon a width of updraft of 2 km. A width of 4.5 km would probably be more appropriate; then $\sigma \approx 0.5\%$ as above. In the case of day 261 of the Atlantic Tropical Experiment (Warner et al. 1980), in a square of side 150 km (of area 22 500 km^2), radar echoes of horizontal area 50 km^2 (width 8 km) at reflectivity 35 dBZ increased in number from 4 to 13 during a period of 2 h: σ increased from 0.9% to 2.9%. A somewhat larger square would probably be appropriate for consideration of radiative–convective equilibrium, yielding smaller values of σ.

The assessments above are quite consistent with the Global Atmospheric Research Program (GARP) Atlantic Tropical Experiment (GATE) studies reviewed by Houze and Betts (1981). Relatively wide updrafts were found in the Tropical Ocean Global Atmosphere Coupled Ocean–Atmosphere Response Experiment (TOGA COARE) case studies by Jorgensen et al. (1997), Roux (1998), and Hildebrand (1998). These may be attributed to large-scale forcing.

For comparison with the above observations, a value $\sigma \approx 0.3\%$ is indicated by the numerical modeling results of Tompkins and Craig (1998). After felicitous choices of horizontal resolution (2 km) and domain size (100 $km)^2$, their results match findings here in many different respects. It seems appropriate to adopt the value $\sigma \approx 0.5\%$ for this study.

A nominal area-wide precipitation rate P is required for conditions of local radiative–convective equilibrium. Figure 7 of Huffman et al. (1997) shows marked variation of P with latitude and season. After Huffman et al., the value $P \approx 1.8$ m $yr^{-1} = 4.9$ mm day^{-1} is adopted for this study, the same as that shown in the model output by Tompkins and Craig (1998). The (100 $km)^2$ domain size of Tompkins and Craig seems just marginally sufficient. The area of deep convective updrafts is then 50 $km^2 = (\pi/4)(8\ km)^2 = 2(\pi/4)(5.6\ km)^2$, enough for one or a few deep cumulonimbus updrafts at a time.

The division of the precipitation rate P by 0.005 to reflect the choice $\sigma \approx 0.5\%$ yields an equivalent local rainfall rate of 40 mm h^{-1} over an area of 50 km^2. Tropical oceanic rain is seen in cells of width ~10 km (area 80 km^2) at radar reflectivity ~35 dBZ (Warner et al. 1980; Jorgensen et al. 1997; Roux 1998; and others). The 35-dBZ reflectivity corresponds to a rainfall rate of about 8 mm h^{-1} (Austin and Geotis 1979; Jorgensen and Willis 1982); a central peak rainfall rate of 46 mm h^{-1} (45 dBZ) is commonly found. Typical rain cells have magnitudes comparable with that obtained here from P and σ.

Energy and entropy budgets are presented in section 2 below. Results from this work are related in section 3 to the finding of a threshold in CAPE by Roff and Yano (2002). Comparison follows in section 4 with results of numerical modeling by Shutts and Gray (1999, hereafter SG). Section 5 is a summary.

2. Energy and entropy budgets

A tropical oceanic domain with the atmosphere above in radiative–convective equilibrium is taken to consist of groups of cumulonimbus clouds with large areas of clear air. The clear areas feature relatively calm seas, and evaporation of moisture into the atmosphere. Under the cumulonimbus, rainfall and gusty winds associated with cold downdrafts occur. The clouds occur in different places in succession over the domain by interaction between radiation, convection, and surface fluxes; by new growth over cold downdrafts (Tompkins and Craig 1998); and by the propagation of gravity waves (Lac et al. 2002). The most common sky condition involves small cumulus and a continuous optically thin high cirrus overcast, as described by Warner and Grumm (1984). See the color graphic Fig. 2 of Pauluis et al. (2000).

In reality it appears that no domain of pure radiative–convective equilibrium ever exists. Deep convection appears always to play a part in the low-level import of energy and the high-level export, as treated in the study by Sui et al. (1994). Here we consider no synoptic-scale forcing, which produces concentrations of deep convective activity. The aim is to estimate, with the aid of observations, the results that should be obtained with a model like that of Tompkins and Craig

Unauthenticated | Downloaded 10/23/21 01:08 AM UTC

TABLE 1. Radiative sources of energy and entropy (see text for explanation).

	Solar	Longwave	Total
	Energy input (W m^{-2})		
To atmosphere	$+Q_{\rm rad}(1-s)$	$-Q_{\rm rad}(1-\upsilon)$	$Q_{\rm rad}(\upsilon-s)<0$
To surface	$+Q_{\rm rad}(s)$	$-Q_{\rm rad}(\upsilon)$	$Q_{\rm rad}(s-\upsilon)>0$
Total	$+Q_{\rm rad}$	$-Q_{\rm rad}$	0
	Entropy input (W m^{-2} K^{-1})		
To atmosphere	$+Q_{\rm rad}(1-s)/T_s$	$-Q_{\rm rad}(1-\upsilon)/T_{\rm l}$	
To surface	$+Q_{\rm rad}(s)/300$	$-Q_{\rm rad}(\upsilon)/300$	

(1998). Diurnal forcing is very strong (Gray and Jacobson 1977); it would be difficult to obtain a meaningful stable simulation if diurnal forcing were to be included.

In a steady-state, evaporation at the surface (at rate E_S) is balanced by precipitation (P). The net influx of solar radiation is balanced by the net efflux of longwave radiation (at rate $Q_{\rm rad}$). The net influx may be taken to occur at a weighted-average, low-tropospheric temperature $T_{\rm short}$, fairly close to the surface temperature T_S, and the net efflux at a weighted-average, midtropospheric temperature $T_{\rm long}$. There is a net radiative export of entropy from the system, $Q_{\rm rad}/T_{\rm long} - Q_{\rm rad}/T_{\rm short} > 0$. This is matched by irreversible production of entropy near the surface and within the atmosphere.

Just above the surface, let the net downwelling solar radiation be $Q_{\rm net\ solar}$. This is a substantial positive quantity, affected by a small surface albedo. Just above the surface, let the net upwelling longwave radiation be $Q_{\rm net\ long}$. There is substantial downwelling longwave radiation, and greater upwelling radiation. With downward fluxes on the left and upward fluxes on the right, all terms being positive, the energy budget per unit area at the surface is

$$Q_{\rm net\ solar} + Pc_{\rm l}T_{\rm rain} = Q_{\rm net\ long} + Pc_{\rm l}T_S + PL_\upsilon(1+\beta). \tag{2.1}$$

Here $c_{\rm l}$ is the specific heat of liquid water and L_υ is the enthalpy (latent heat) of evaporation at the surface at temperature T_S. The symbol β refers to the Bowen ratio of sensible heat flux to evaporation heat flux. It has a small positive value, enhanced because of heat transfer to downdraft air at the surface under the cumulonimbus. The term $Pc_{\rm l}T_{\rm rain}$ is the flux of enthalpy of rain falling out of the atmosphere at temperature $T_{\rm rain}$, a few degrees lower than T_S. The terms $Pc_{\rm l}T_S + PL_\upsilon$ represent the enthalpy flux of evaporating moisture. The term βPL_υ is the sensible heat flux from the surface. The term $Pc_{\rm l}(T_S - T_{\rm rain})$ is small, so

$$Q_{\rm net\ solar} \approx Q_{\rm net\ long} + PL_\upsilon(1+\beta). \tag{2.2}$$

The balance of entropy fluxes at the surface is given by

$$Q_{\rm net\ solar}/T_S \approx Q_{\rm net\ long}/T_S + PL_\upsilon(1+\beta)/T_S. \tag{2.3}$$

For the system as a whole, the net radiative export of entropy, $Q_{\rm rad}/T_{\rm long} - Q_{\rm rad}/T_{\rm short}$, is balanced by irreversible sources of entropy close to the surface and within the atmosphere. There are irreversible sources due to the following: dissipation of kinetic energy, the work done by falling precipitation, diffusion of water vapor close to the sea surface, evaporation of the condensate, mixing of air parcels of different temperature and moisture content, diffusion of sensible heat (in particular through the first few meters above the surface), and the generation of gravity waves. For the system as a whole, the net export of entropy by radiation is written on the left of the balance. The irreversible generation terms are written on the right, expressed in the order listed above. Symbols and derivations are explained in the following paragraphs:

$$Q_{\rm rad}/T_{\rm long} - Q_{\rm rad}/T_{\rm short} = D_K/T_K + gPz_P/T_P - PR_\upsilon \ln H_S - P(1/\varepsilon_P - 1)R_\upsilon \ln H_P + \Delta S_{\rm mixing} + (\beta PL_\upsilon)\Delta T T_S^{-2} + D_G/T_G. \tag{2.4}$$

a. Radiative export of entropy

Budgets of the energy and entropy of radiation for the whole globe have been treated by Goody (2000). Table 1 is an algebraic version of Goody's Table 3. The fraction s describes the relative amount of solar radiation that is absorbed at the surface at a temperature of 300 K, as opposed to absorption in the atmosphere at weighted temperature T_s. The fraction υ describes the relative amount of longwave radiation emitted at the surface that reaches space, as opposed to emission from within the atmosphere at weighted temperature $T_{\rm l}$. There is balance of energy absorption and emission, with a net production of entropy. The total entropy production EP is given by

$$\mathrm{EP} = Q_{\rm rad}[(s-\upsilon)/300 + (1-s)/T_s - (1-\upsilon)/T_{\rm l}] < 0, \tag{2.5}$$

rather than zero as for the energy. The quantity $Q_{\rm rad}(s - \upsilon)$ is equal to the surface heat flux $PL_\upsilon(1+\beta) =$

Unauthenticated | Downloaded 10/23/21 01:08 AM UTC

153 W m^{-2}. In their study, PH gave this quantity as 157.4 W m^{-2}. Tompkins and Craig (1998) had Q_{rad} = 287 W m^{-2}. They gave the albedo as 0.18. This matches a combination of 20% cloudy atmosphere with an albedo of 0.65 (Peixoto and Oort 1992) and 80% clear atmosphere with an albedo of 0.06. Study of the combinations of "cirrus" and "clear-sky" conditions treated by Stephens and O'Brien (1993, their Table 1) indicates that in these circumstances, the 287 partitions as 23 for the cloudy areas and 264 for the clear areas: the clear areas dominate. Then with fractions and temperatures appropriate for clear air, and $T_1 \approx T_s = T$, Eq. (2.5) may be rewritten as

$$\mathrm{EP} \approx Q_{rad}(s - \upsilon)(1/300 - 1/T) < 0. \tag{2.6}$$

The fraction $(s - \upsilon) \approx 153/287 = 0.53$. Figure 3a of Stephens and O'Brien (1993) suggests that $T \approx 273$ K. Rennó and Ingersoll (1996, their Table 2) assumed a surface heat flux of 155 W m^{-2}, a surface temperature of 299 K, and $T = 269$ K. Then $-\mathrm{EP} = 50$ or 58 mW m^{-2} K^{-1}, respectively. This estimate is very uncertain. Variable in space and time, EP is a small difference between large terms and very sensitive to the various relevant parameters. The values obtained are somewhat smaller than results from Goody (2000) for the whole globe, ≈72 mW m^{-2} K^{-1}. The alternative device $(Q_{rad}/T_{long} - Q_{rad}/T_{short})$ in (2.4) = –EP = 54 if T_{long} = 271 K and T_{short} = 285.5 K.

b. Mechanical dissipation, D_K/T_K

After presenting the kinetic energy equation for the atmosphere, EB showed that in the absence of all the other irreversible terms on the right-hand side of the entropy balance, the mechanical dissipation D_K, occurring at representative temperature T_K, is equal to the work due to pressure (p) performed by the convecting circulation of velocity **V**. For a closed system, this may be written as

$$D_K = \int_{\mathrm{Volume}} p\nabla \cdot \mathbf{V}. \tag{2.7}$$

In the absence of the other sources of dissipation, the pressure work represents potential energy available for conversion to kinetic energy. In their study, EB showed that the pressure work is close to the net vertical buoyancy flux:

$$D_K = \int_{\mathrm{Volume}} g(\rho - \overline{\rho})w, \tag{2.8}$$

where w is the vertical air velocity, ρ is the density, and $\overline{\rho}$ is the horizontal mean of the density. At the end of their paper they reviewed the assumption that D_K/T_K is the only dissipative term of note and concluded that the mechanical dissipation D_K might yield 50% of the total irreversible entropy production. More recent work has shown that D_K is much less than this.

For the whole globe, Goody (2000) estimated the total entropy source due to dissipation of momentum at 11.3 mW m^{-2} K^{-1}. Of this, 6.0 mW m^{-2} K^{-1} arises from stress in the boundary layer, which increases with the cube of wind speed. Goody took the wind speed as 10 m s^{-1}. A speed of 3.7 m s^{-1} is more appropriate for the generally light and variable winds to be expected here: this estimate comes from approximate area weightings from Fig. 5 of Tompkins and Craig (1998): $15\%(6)^3 + 65\%(3)^3 \approx (3.7)^3$. Then the contribution due to surface stress is 0.2 mW m^{-2} K^{-1}. In their study, PH also found that this term is small.

In terms of turbulent air motion, the mechanical dissipation D_K may be assessed as a typical rate of dissipation ε_K per unit mass of turbulent kinetic energy (TKE):

$$D_K \approx \rho\varepsilon_K H\sigma, \tag{2.9}$$

where H is the height of the convective column and σ is the fractional area coverage (section 1b). It is assumed that

$$\varepsilon_K \approx 2w_*^3 W^{-1}, \tag{2.10}$$

$$\varepsilon_K \approx W^2 t_W^{-3}, \tag{2.11}$$

where w_* is a convective scale velocity, W is a typical width of a cloud tower, and t_W is the lifetime before dissolution commensurate with the width W [after Baker et al. (1984), their Eqs. (2) and (5), respectively. They were considering shear like $w_*/(W/2)$. They dropped a factor of 3/2 in their Eq. (5); here this 3/2 is retained]. Consistent with the findings of Zipser and LeMone (1980), Lucas et al. (1994), and others, Warner and McNamara (1984) found that mean updraft velocities in smaller cumulus are remarkably constant, near 2.5 m s^{-1}. Rise rates of tropical oceanic cumulus clouds in the high troposphere are often near 8–9 m s^{-1} (Houze and Betts 1981; Warner and Grumm 1984). Warner and McNamara found that a typical vertical velocity of 2.5 m s^{-1} is commensurate with a typical width of 1400 m. Then Eq. (2.10) yields $\varepsilon_K \approx 0.02$ m^2 s^{-3}. After (2.11) the lifetime of a turbulent convective updraft of depth $H \approx 10$ km is assessed as $(H^2/\varepsilon_K)^{1/3} \approx 28$ min; this result is compatible with the histories of radar echoes shown by Warner et al. (1980). Warner et al. (1973) studied small elements of clouds on the tops of an Alberta hailstorm, and found that they featured a median width of 150 m and lifetime of 1.3 min. The dissipation rate ε_K from (2.11) then amounts to 0.05 m^2 s^{-3}. Another such storm yielded a similar result. Hailstorms are more energetic than cumulus clouds over tropical oceans. The value 0.02 m^2 s^{-3} (=72 J kg^{-1} h^{-1}) is taken as a general representation for the present case, in view of the dominance by active cloud towers found from exploration by aircraft.

With $\varepsilon_K \approx 0.02$ m^2 s^{-3}, the depth of turbulent convection $H \approx 10$ km, $\rho = 0.7$ kg m^{-3} and $\sigma = 0.005$,

Unauthenticated | Downloaded 10/23/21 01:08 AM UTC

Eq. (2.9) yields $D_K \approx 0.7$ W m^{-2}. With $T_K = 268$ K, $D_K/T_K \approx 2.6$ mW m^{-2} K^{-1}. Adding the contribution of surface stress, the total of D_K/T_K is 2.8 mW m^{-2} K^{-1}.

c. Dissipation D_P/T_P due to falling precipitation

Pauluis et al. (2000) wrote about the frictional dissipation D_P due to precipitation falling at weighted temperature T_P. They stated that "this interaction performs mechanical work at a rate $\mathbf{F} \cdot (\mathbf{V} + \mathbf{V_T})$ on the drops and $\mathbf{F} \cdot \mathbf{V}$ on the air parcel." Here $\mathbf{F}$ is the frictional force between raindrop and air, $\mathbf{V}$ is the air velocity, and $\mathbf{V_T}$ is the fall velocity of the raindrops relative to the air. The term $\mathbf{F} \cdot \mathbf{V}$ represents the *passive* effect of water loading on air density; only the term $\mathbf{F} \cdot \mathbf{V_T}$ represents an interaction. Both of the terms $\mathbf{F} \cdot \mathbf{V}$ and $\mathbf{F} \cdot \mathbf{V_T}$ are dissipative, and their sum correctly represents the overall effects of falling rain. The force balance is between the weight of the hydrometeors and the viscous drag, to a close approximation [Bannon 2002, after his Eq. (5.11)]. In this case the rate of loss of gravitational potential energy of a falling drop is $\mathbf{F} \cdot (\mathbf{V} + \mathbf{V_T})$. The first term has to be separated from the second and treated in terms of air density. In his Eqs. (6.8) and (6.9), Bannon shows that the work interaction between drops and air is a positive definite contribution to internal energy, confirming the conclusion of Pauluis et al. (2000).

The mechanical work $\mathbf{F} \cdot \mathbf{V_T}$ is a function of the Reynolds number $\mathrm{Re} = V_T\, d/\nu$, where d is the drop diameter, ν is the kinematic viscosity, and V_T is the magnitude of $\mathbf{V_T}$. This term may be partitioned into two components. Imagine a drop gradually growing from nothing to a size commensurate with Re = 400 ($d \approx 1.3$ mm), then diminishing again to nothing. At all times let its weight be balanced by the drag. The drag is partitioned using a form drag coefficient and a friction drag coefficient, the sum of which is the total drag coefficient. Form drag is related to the difference in pressure vertically across the falling drop, which acts to force the air downward. Both form drag and frictional drag are dissipative; the former is distinguished in that it constitutes a direct forcing of the air circulation, as does the term $\mathbf{F} \cdot \mathbf{V}$. Data on the drag coefficients are given by Le Clair et al. (1970). At very small sizes frictional dissipation dominates, and the total drag coefficient is very large. As Re increases from 0.01 to 5 the ratio of form drag to frictional drag is near 0.5, and the total drag coefficient decreases to about 7. At Re = 200 the two forms of drag are about equal; the total drag coefficient is 0.77; at Re = 400 the total drag coefficient is 0.55—now only slowly decreasing. One infers that the ratio of drag coefficients continues to rise slowly from 1.4. At Re > 400, vortex shedding in the wake of the drops may alter this scenario (Pruppacher and Klett 1997), but it seems safe to infer that form drag and frictional drag are comparable for raindrops. Rennó (2001) gives a broadly similar account. For typical rain approaching the surface, with largest drops of diameter roughly 3 mm falling at about 9 m s^{-1}, with Re $\approx$ 1500 and the drag coefficient roughly at 0.4, it seems appropriate to partition the work $\mathbf{F} \cdot \mathbf{V_T}$ equally into one-half related directly to the generation of kinetic energy and the other half to losses.

The work rate per unit surface area D_P is obtained by integrating the work rate $\mathbf{F} \cdot (\mathbf{V} + \mathbf{V_T})$ over all drops over that unit area. This is equal to gPz_P, where g is the gravitational acceleration and z_P is the precipitation pathlength through the depth of the atmosphere (Pauluis et al. 2000). The associated irreversible entropy source is gPz_P/T_P. The pathlength z_P is set to 8 km, after Pauluis et al., who indicate 5–10 km, and the temperature T_P is set to 280 K. The gravitational acceleration $g = 9.8$ m s^{-2}. Then $gPz_P/T_P \approx 16$ mW m^{-2} K^{-1}. Taking account of the prevalence of small hydrometeors at high altitudes, a fraction $0.6V_T/(V + V_T)$ of this quantity is taken to represent losses, and the remainder is taken to contribute directly to the generation of kinetic energy of the convective circulation. Guidance as to V_T comes from Warner et al. (1980), whose radar wall chart shows that the fall speed of precipitation patterns, indicative of $(V + V_T)$, reaches roughly 12 m s^{-1}. Hildebrand (1998) indicates that relevant values of V are not strong over the open ocean. Taking $V \approx 0.25\, V_T$, the fraction of losses $0.6V_T/(V + V_T) \approx 0.5$, so about 50% of the work rate of precipitation directly generates kinetic energy. To estimate uncertainties, the factor 0.6 is varied in the range 0.5–0.8 and V/V_T in the range 0.2–0.4. Then the 50% for direct generation of kinetic energy is in the range 33%–71%. There are many subtleties, for instance partial re-evaporation of condensate, and comprehensive numerical modeling should be undertaken.

The dissipation rate D_K may be regarded as potential dissipation, which will occur sometime after the corresponding winds of the direct circulation have been generated by the conversion of available potential energy (APE). On the other hand, the downdrafts induced by rain are considered as part of the process of losses to this APE and so might warrant independent consideration (Goody 2003). However there is no way of separating these wind components, which are linked by mass continuity. There is no mathematical basis (like Helmholtz's theorem) for separating them; nor could they be distinguished by measurements, for instance by means of roving aircraft.

Downdrafts accompanying rain at the surface are commonly found to be cold due to evaporation, which is considered next.

d. Diffusion following evaporation at the surface, $-P\, R_v\, lnH_S$

Following PH, the irreversible entropy source related to evaporation at the surface is $-P\, R_v \ln H_S$, where H_S is the relative humidity at the surface. The gas constant for water vapor $R_v = 461$ J kg^{-1} K^{-1}. The relative

Unauthenticated | Downloaded 10/23/21 01:08 AM UTC

humidity H_S at the surface is set to 80% (after observations by Kley et al. 1997). Then for the surface evaporation, $-P\ R_v\ \ln H_S \approx 5.9$ mW m^{-2} K^{-1}.

e. Evaporation of precipitation, $\Delta S_{pptn} = -P(1/\varepsilon_P - 1)\ R_v\ lnH_P$

Let C denote the total rate of condensation within the atmospheric circulation. In their study, PH defined the precipitation efficiency ε_P as the ratio P/C and gave the value 27%. So $C = P/\varepsilon_P \approx 3.7\ P$ is a large quantity. The value 27% is at the low end of the range of efficiencies from 20% to 53% (dependent upon convective intensity and wind shear) reviewed by Shie et al. (2003): All of these efficiencies are from two-dimensional models, and are probably overestimates because spreading of condensate in three dimensions is not allowed. Results presented from their three-dimensional modeling by Tompkins and Craig (1998) allow an estimate of their precipitation efficiency: Their $P = 4.9$ kg m^{-2} day^{-1}, the same as is assumed here. They show a peak upward mass flux at the cloud base of 0.0095 kg m^{-2} s^{-1}, with mixing ratio of water vapor of about 0.0165. Then, $\varepsilon_P \approx 36\%$. This value seems satisfactory for the present purpose. It seems quite high for a three-dimensional model, but there is likely to be no great reduction due to spreading of precipitation by wind shear.

The condensation C is equal to the sum of precipitation and evaporation within the atmosphere (E_A):

$$C = P + E_A. \tag{2.12}$$

Therefore,

$$E_A = P/\varepsilon_P - P \approx 1.8P. \tag{2.13}$$

The irreversible entropy source due to evaporation (E_A) within the atmosphere is then given by

$$\Delta S_{\text{pptn}} = -P(1/\varepsilon_P - 1)R_v \ln H_P, \tag{2.14}$$

where H_P is the weighted average relative humidity at which the precipitation evaporates. Precipitation efficiency less than 1 implies recycling of moisture within the atmosphere and associated energy costs of irreversible entropy production.

The magnitude of the evaporation term is sensitive to the relative humidity H_P. Cirrus effluent is commonly carried hundreds of kilometers downwind from its source in long plumes readily seen in satellite pictures (Scorer 1986). Ice crystals fall from these plumes downward several kilometers, evaporating as they go. Braham and Spyers-Duran (1967) found ice crystals at 500 hPa fallen through dry air from levels near 250 hPa. They pointed out that for an ice crystal, "the rate of mass loss is directly proportional to the difference in vapor concentration between a crystal and its environment. Because of the very low temperatures at cirrus levels, the total capacity of space for water vapor is small. . . . The survival of cirrus crystals is much more sensitive to the humidity at $-10°$ and $-20°$C levels than it is to the humidity at the cirrus levels." In their study of small ice crystals at altitudes near 15–16 km, Comstock et al. (2002) noted in one instance that "layer heating does not appear to be contributing to significant ice evaporation." For an assessment of the relative humidity relevant to the gradual evaporation of cirrus, we look at values just below plume levels. Over the central equatorial Pacific, Kley et al. (1997) found that areas under the influence of active deep convection featured relative humidities in excess of 75% over most of the troposphere. Data given by Sherwood (1996, his Fig. 3a) are in agreement. However, values under 60% in active areas are sometimes found, and the high values probably reflect the fact that evaporation has already taken place. Calculations by Heymsfield and Donner (1990, their Fig. 8) show that evaporation of ice crystals is slow unless the relative humidity is 60% or less. The conclusions here are supported by the modeling results of Tompkins and Craig (1998): They found substantial convective downdrafts descending to an altitude of 8 km, through air of domain-average relative humidity of about 40%. For the lower troposphere relevant for the evaporation of rain, it appears from both observations and modeling studies that 80% is a representative value of relative humidity.

It is supposed that one-third of the evaporation occurs in the upper to middle troposphere where the relative humidity is ~60%, and the other two-thirds in the lower troposphere at relative humidities near 80%. These values are somewhat larger than those shown in Fig. 9 of Tompkins and Craig (1998), and closer to those of Iwasa et al. (2002). The precipitation efficiency ε_P is set to 0.36. Then for the evaporation of precipitation $-P(1/\varepsilon_P - 1)\ R_v \ln H_P \approx 15$ mW m^{-2} K^{-1}. (If ε_P is taken as 27% and H_P as 60%, then the 15 becomes 36 mW m^{-2} K^{-1}; the uncertainty is large). This entropy source is substantially greater than the entropy source due to evaporation at the surface, $-P\ R_v\ \ln H_S$.

f. Mixing, ΔS_{mixing}

It is necessary to consider the irreversible production of entropy ΔS_{mixing} of air parcels of different temperature and composition. In their study, EB estimated that for mixing of saturated air in updrafts with environmental air, the irreversible entropy production amounts to roughly 5% of the total irreversible entropy production. We note after PH that the local dispersion of water vapor that occurs immediately after evaporation is catered for under the evaporation of precipitation. Isobaric mixing is considered, at constant aggregate enthalpy, of unsaturated parcels of air on scales of hundreds or thousands of meters, over times on the order of an hour. This is expected to result from cloud system propagation, and a proliferation of thin stratiform "shelf clouds" arising from cumulus (Ludlam 1980; Warner 1984b), with consequent changing fluxes of ra-

Unauthenticated | Downloaded 10/23/21 01:08 AM UTC

diation. The following formula may be derived for the mixing of two unsaturated parcels of equal mass, one with temperature $T+T'$ and specific humidity $q+q'$, and the other with similar anomalies of opposite sign. Per unit mass and time

$$\Delta S_{\text{mixing}} \approx \tfrac{1}{2}c_{pd}(T'/T)^2 - (c_{pv} - c_{pd})q(q'/q)(T'/T) + \tfrac{1}{2}R_v q(q'/q)^2, \quad (2.15)$$

where the specific heats at constant pressure c_{pd} and c_{pv} refer to dry air and water vapor, respectively, and R_v is the gas constant for water vapor. Suppose that a large fraction of the troposphere is involved in this mixing, 4090 kg m^{-2} (400 hPa), and that the mixing takes 3.6 ks. Let the mixing be represented by $q \approx 0.008$, $(T'/T) \approx (0.5/268)$, and $(q'/q) \approx (-1/20)$. Then the three terms in (2.15) become

$$\Delta S_{\text{mixing}} \approx 2.0 + 0.7 + 5.3 = 7.9 \text{ mW m}^{-2} \text{ K}^{-1}. \quad (2.16)$$

This is a substantial contribution; it is very sensitive to the assumptions. The distribution of q shown in Fig. 3 of the model output by Iwasa et al. (2002) suggests that the (q'/q) value might be rather small. Many are the ways in which uncertainties could be explored; the matter will not be pursued further here. This source is the area of greatest ignorance in this investigation. Following PH, related irreversible entropy production due to thermal diffusion, calculated in the manner of the next section, will be taken as small and ignored.

Common observation while flying past cirrus, or records of such views afforded by stereo-pair photographs such as Warner (1984b, Fig. 6, or Fig. 2 below) suggest that substantial mixing occurs in relation to contrasts engendered by evaporation, at small scales difficult to treat by numerical modeling.

g. Dissipation (βPL_v) $\Delta T\ T_S^{-2}$ related to the surface sensible heat flux

In terms of the surface sensible heat flux (βPL_v), this term, (βPL_v) $\Delta T\ T_S^{-2}$, is due to turbulent diffusion from the surface at temperature T_S to a level a few meters above where the temperature is $T_S - \Delta T$ [PH, their Eq. (17)]. The enthalpy of evaporation $L_v = 2440$ kJ kg^{-1} K^{-1}. Let $T_S = 300$ K, and suppose that diffusion occurs through a temperature difference $\Delta T = 1$ K. The value 0.1 is often quoted as an average value for the Bowen ratio β over tropical oceans (Pond et al. 1971). There is some enhancement in disturbed conditions (Geldmeier and Barnes 1997; Jorgensen et al. 1997). The choice $\beta \approx 0.1$ is consistent with the recent review by Garstang and Fitzjarrald (1999). Then (βPL_v) $\Delta T\ T_S^{-2} \approx 0.16$ mW m^{-2} K^{-1}. This term is small, as stated by EB and PH. For the whole globe, Goody (2000) reported the result from the Goddard Institute for Space Studies (GISS) model as 5% of the total or 3.4 mW m^{-2} K^{-1}. Greater thermal contrasts at high latitudes than in the Tropics are responsible for the difference.

h. Dissipation associated with gravity waves

It is difficult to give an appropriate assessment of the dissipation associated with the generation of gravity waves by disturbances in stable strata of the atmosphere by rising cumulus towers. In their numerical modeling work Lac et al. (2002) demonstrated the importance of deep, fast-moving modes for regeneration of mesoscale convective systems. They did not give details of short, slow-moving gravity waves.

Lane et al. (2001) gave details of the mechanisms of generation of gravity waves by penetrative cumulus towers. They modeled deep convection over the Tiwi Islands off northern Australia, where heated land surfaces enhance deep convection. They found that work done by rising towers (as opposed to differential heating or environmental flow over such towers) was the dominant source of energy of gravity waves, and that the largest amplitude gravity waves are generated when cloud tops reach the upper troposphere. The tropopause was at 16 km. They were chiefly interested in propagation of wave energy into the stratosphere. Their calculated waves were remarkably monochromatic with a horizontal wavelength of about 17 km, and no preferred direction of propagation. The reports of both Lac et al. and Lane et al. imply that the energy of short, slow-moving gravity waves is small.

Pfister et al. (1993) recorded observations from aircraft over anvils at the tropopause at altitude 17.3 km over the Gulf of Panama. They found that vertical excursions of air in the stratosphere probably related to gravity waves were of amplitude roughly 200 m. Such high altitudes of the tropopause and of anvils from cumulonimbus are generally associated with the proximity of land surfaces and are of limited occurrence (Gettelman et al. 2002). The equilibrium scenario treated here is regarded as midoceanic and the convection is gentler than that examined by Pfister et al. and Lane et al. (2001).

A simple estimate may be made of the amount of work done by a rising cloud tower in lifting a body of dry air upward from the tropopause into the stratosphere [of lapse rate (2.5 K)/(15 hPa)], which can be expected to lead to mechanical dissipation related to gravity waves. To convert the work into an appropriate quantity of dissipation, we multiply by an inverse Reynolds number. In their realistic simulations of nonprecipitating and sustained cumulus congestus clouds, Carpenter et al. (1998) used an eddy viscosity related to a coefficient $C_K \approx 0.094$, and this is taken as the appropriate inverse Reynolds number. If the volume of air is in the form of a spherical cap of maximum thickness 5 hPa, and if it is lifted through 11 hPa, a displacement commensurate with the findings of Pfister et al. (1993), then with fractional area coverage $\sigma \approx 0.005$ and with

Unauthenticated | Downloaded 10/23/21 01:08 AM UTC

TABLE 2. Irreversible entropy source terms. See text for details of source terms. Estimates of magnitudes come from Goody (2000; the GISS model) and PH. After a comma, percentages are sometimes followed by the corresponding flux in mW m^{-2} K^{-1}. Under columns 3 and 4 the percentages between dashes cover all the terms not specified elsewhere. Under the "Conclusions" are best estimates based on all the evidence considered, as a percentage of the whole and in mW m^{-2} K^{-1}. Assignment of a representative temperature in the next column allows assessments of components of dissipation (W m^{-2}), to be compared with PH in the last column.

Entropy source term		GISS mW m^{-2} K^{-1}	PH	Conclusions mW m^{-2} K^{-1}	Temperature K	Dissipation PH W m^{-2}	W m^{-2}
Mechanical	D_K/T_K	16%, 11.5	4%	5.2%, 2.8	268	0.75	1.0
Falling precipitation	gPz_P/T_P		30%	30%, 16	280	4.5	3.7
Surface evaporation	$-P\,R_v \ln H_S$			11%, 5.9	300	1.8	0.6
Evaporation of precipitation	$-P(1/\varepsilon_P - 1)\,R_v \ln H_P$			37.5%, 20	280	5.6	
		— 79%, 57.9	66%—				8.3
Mixing	ΔS_{mixing}			15%, 8	268	2.1	
Gravity waves	D_G/T_G			0.9%, 0.5	268	0.13	0
Surface sensible heat flux	$(\beta P L_v)\,\Delta T\,T_S^{-2}$	5%, 3.4	Small	0.4%, 0.2	300	0.06	0
Totals		100%, 72.8	100%	100%, 53.4	279	14.9	13.6

one tower appearing every 25 min (Warner et al. 1980), an average dissipation rate D_G may be determined. Division of this rate by the tropopause temperature 188 K yields the rate of irreversible production of entropy $D_G/T_G \approx 0.2$ mW m^{-2} K^{-1}, a small amount. This crude treatment may be compared with an instant answer as follows.

Kershaw (1995) found in his numerical simulations that the energy density of a gravity wave could be linked by an efficiency with the energy density of convective motions, and obtained a value of 0.18 for this efficiency. If we simply write $D_G/T_G \approx 0.18\,D_K/T_K$ with $D_K/T_K \approx 2.6$ mW m^{-2} K^{-1} after section 2b above, then $D_G/T_G \approx 0.5$ mW m^{-2} K^{-1}, not far from the value obtained above. For the unforced midoceanic regime considered here, this assessment seems appropriate.

i. Collection and comparison of assessments

The contributions assessed in the paragraphs above are collected in Table 2. Pairs of numbers in Table 2 show percentages of the total irreversible entropy production, and corresponding quantities (in the units mW m^{-2} K^{-1}). Goody (2000) presented his own assessments of global averages, and like results from the GISS general circulation model. Goody neglected the evaporation of precipitation. In other respects his results were like those from GISS, so in Table 2 just the global GISS model results are presented. After Goody's Table 7 we have 16% (11.5 mW m^{-2} K^{-1}) for mechanical dissipation, 5% (3.4 mW m^{-2} K^{-1}) for dry convection and 79% (57.9 mW m^{-2} K^{-1}) for moist convection, with -72.8 mW m^{-2} K^{-1} for the net radiative flux divergence.

The results under PH in Table 2 come after the energy budget (Table 4) of PH. They attributed 30% of the total irreversible entropy production to falling rain. Their Table 4 indicated 4% for frictional dissipation. They gave 60% for irreversible phase changes and diffusion of water vapor. This leaves 6%, which is added to the 60% to cover all of the unspecified terms in Table 2.

Under "Conclusions" in Table 2 the mechanical term is assessed as 2.8 mW m^{-2} K^{-1}, much smaller than the amount indicated under GISS. The next figures in mW m^{-2} K^{-1} follow from the paragraphs above. For the evaporation of precipitation 20 mW m^{-2} K^{-1} is adopted, rather than 15 as found first in section 2e. It is difficult to assess the term ΔS_{mixing}. In their paper, EB found that roughly 5% of the total irreversible production of entropy was due to saturated parcels mixing into the local environment. With the effect tentatively quantified in section 2f above, 8 mW m^{-2} K^{-1} appears to be roughly appropriate. Then the total amounts to 53 mW m^{-2} K^{-1}, in broad agreement with results in section 2a. The contribution of sensible heat is much larger in the global context (GISS) than for the Tropics. For the sum of the evaporation and mixing terms 66% is found from PH, in agreement with the 63.5% found here.

Averaging to arrive at the estimates in Table 2 is over phenomena ranging over orders of magnitude. The uncertainties in the budget of irreversible sources of entropy may be considered with the aid of a bar chart (Fig. 1). The vertical extent of the chart is commensurate with the total of irreversible sources of entropy, 53.4 mW m^{-2} K^{-1}. This total is uncertain. The term labeled MECH represents the sum D_K/T_K plus the small contribution D_G/T_G in Table 2. It is sensitive to both the fractional area coverage by deep convective updrafts, and the rate of dissipation of turbulent kinetic energy, both of which are uncertain. The fractional area coverage depends upon the synoptic-scale forcing to which convection is responding—none in this scenario. The term might be 2 or 3 times larger than represented, or smaller. The term SFC encompasses both the evaporation and the small effect of sensible heat flux. The term PPTN EVAP depends upon both precipitation efficiency and relative humidity. The PPTN LOAD term also needs detailed study. The three middle bars in Fig. 1, amounting to 79% of the total, are proportional to the rate of precipitation P, so they would go up or down in concert with P. Finally, the mixing term

Unauthenticated | Downloaded 10/23/21 01:08 AM UTC

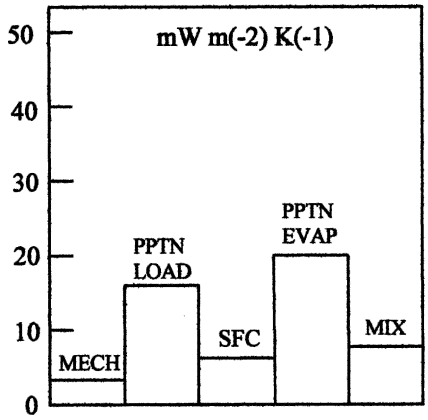

FIG. 1. Bar chart of individual terms in the budget of irreversible sources of entropy in Table 2. The vertical extent is commensurate with the total, 53.4 mW m^{-2} K^{-1}. See text for further details.

(MIX) is found to be large. It might be overestimated if the bulk of the atmosphere heats and cools in response to changes of radiation by spreading anvil and shelf clouds without much mixing, but this seems unlikely. Underestimation is also possible. The MIX and PPTN EVAP terms contribute the greatest uncertainties to the overall budget, while the magnitude of the MECH term with respect to the whole is also very uncertain. The budget presented is for a hypothetical case with no forcing other than radiation. It is an exploration of the relative magnitudes of the different terms, with the necessity for internal consistency in mind.

A stereo-pair of cloud photographs is shown in Fig. 2. Most of the low clouds were over land surfaces of the east coast of Borneo. The photographs indicate that there was little shear of the wind through the upper half of the troposphere. Consider the three largest terms in Table 2: Falling precipitation is hidden from view. Evaporation of hydrometeors is suggested by the diffuse and indented character of the upper cloud boundaries shown in Fig. 2; implied is a substantial thermal contrast between the air overshadowed by dense high overcast at right in the view, and adjacent clear air. In open ocean conditions, tall clouds like these would propagate: Substantial mixing, concentrated locally, is to be expected.

In the last two columns of Table 2 the individual irreversible source terms of entropy are expressed as rates of dissipation (W m^{-2}). Entries in the last column are from PH. For this purpose, in the column third from last, representative temperatures of 280 K for evaporation of precipitation (after Fig. 6 of PH) and 268 K for mixing are assigned. The total dissipation then amounts to 14.9 W m^{-2}. (Combination of this with the total entropy source 53.4 mW m^{-2} K^{-1} yields the overall

FIG. 2. Stereo-pair of photographs illustrating equatorial convection, partly related to underlying coastal topography, taken by the author from 1.0°S, 109.3°E, 500 hPa at 0753 UTC on 6 Dec 1978, looking northward. The photographs are mounted with the right-eye view on the left and vice versa, for cross-eye viewing (Warner 1984b, 2003).

Unauthenticated | Downloaded 10/23/21 01:08 AM UTC

representative temperature 279 K.) In their study, PH showed a slightly greater mechanical dissipation (1.0 W m^{-2}) than the present value 0.75 W m^{-2}. They gave 3.7 and 0.6 for falling precipitation and surface evaporation, as opposed to 4.5 and 1.8 W m^{-2}. For the sum of evaporation of precipitation and mixing, PH gave 8.3 W m^{-2}. This is close to the sum 5.6 + 2.1 W m^{-2} obtained here. The total from PH, 13.6, is close to the present 14.9 W m^{-2}.

How much of the dissipation is associated with generation of the direct convective circulation? After sections 2b and 2c, this is taken as all of the mechanical term and 50% of the falling precipitation term. Division by the sum of latent and sensible heat fluxes at the surface then yields the efficiency η_S:

$$\eta_S = [D_K/T_K + 0.5(gPz_P/T_P)]/[PL_v(1 + \beta)]. \quad (2.17)$$

The sum 0.75 + 0.5(4.5) = 3.0 W m^{-2}. Division by 153 W m^{-2} yields $\eta_S \approx 2.0\%$. To estimate uncertainties, the 0.75 is varied by a factor of 3, and the factor 0.5 from 0.33 to 0.71 (section 2c). Then η_S varies between 1.1% and 3.6%. Convection lifts up water substance: some of it rapidly falls and drags air down with it. The mature convective circulation is driven partly by downdrafts, linked to updrafts by mass continuity. As found also by PH, the mechanical term D_K/T_K is small. It contributes 25% (7.3% to 60%) to the efficiency η_S. This means that η_S is relatively insensitive to the precipitation rate.

3. On the work of Roff and Yano (2002)

Roff and Yano (2002) calculated CAPE over the west Pacific warm pool. They distinguished pCAPE obtained from following a parcel up a pseudoadiabat to the level of neutral buoyancy (LNB) from rCAPE obtained by following a reversible adiabat (with no freezing). In cases of small pCAPE they found that rCAPE could be near zero or negative, and that above a threshold of pCAPE (≈1100 J kg^{-1}), pCAPE and rCAPE rose in concert (see their Fig. 1). In calculations of pCAPE, rising parcels end up at the LNB with almost no moisture. In calculations of rCAPE parcels contain as much water as they had at cloud base. In cases of deep convection the difference (pCAPE − rCAPE) is thus related to $g\,q_T\,H$, where g is the acceleration of gravity (9.8 m s^{-2}), q_T is the mean specific humidity of condensate in the rising column (~0.012 in active tropical cases examined by the author), and H is the depth of the convecting layer (15 km); so $(g\,q_T\,H) \approx 1800$ J kg^{-1}. The author finds that $(g\,q_T\,H)$ yields overestimates of the difference (pCAPE − rCAPE) for tropical cases featuring substantial instability, and that (pCAPE − rCAPE) ≈1100 J kg^{-1}, the same as the threshold found by Roff and Yano. The difference (pCAPE − rCAPE) appears to be proportional to about 11/18 (≈60%) of the quantity $(g\,q_T\,H)$. It seems that the threshold found by Roff and Yano may be commensurate with the energy (as measured by pCAPE) required to support a column of precipitation, and thus to initiate a local deep convective circulation. Roff andYano suggested this, but invoked the full magnitude of $(g\,q_T\,H)$. The importance of precipitation found by PH, confirmed in section 2, is consistent with this inference.

4. Comparison with the work of Shutts and Gray (1999)

In their study, SG treated a condition of radiative–convective equilibrium by means of a three-dimensional numerical model. They considered a polar airstream flowing at 10 m s^{-1}, with forcing by radiative cooling stronger than the case considered in section 2. With their strongest forcing, their rainfall was about 6 m yr^{-1}, as opposed to $P = 1.8$ m yr^{-1} in section 2. After their numerical model results, SG reviewed previous theoretical work by RI, EB, and Craig (1996).

Equation (7) of SG reads

$$\alpha F_h \approx M_c \Delta\text{MSE}. \quad (3.1)$$

Here α (=0.666) refers to the fraction of the total energy sink that occurs in the deep convecting layer, F_h is the total surface energy flux, M_c is the mean mass flux carried by convective updrafts, and ΔMSE is the difference in moist static energy between updraft and environment at the level of the MSE minimum. This equation resembles the combination (20) and (21) of RI, and (23) of EB. We also have Eq. (26) of SG:

$$M_c \approx \rho\sigma w_*, \quad (3.2)$$

which relates the mass flux to the mean density ($\rho \approx$ 0.71 kg m^{-3}), the mean fractional updraft area σ, and the characteristic updraft velocity w_* [cf. Eqs. (22) of RI and (2) of EB]. From their Eqs. (16)–(19), SG calculated the efficiency η and the corresponding dissipation rate D_{tot} from the mean buoyancy flux, related to surface parameters and the depth of the convecting layer. This is comparable with η_k of PH. From their Eqs. (9)–(13) SG calculated $\eta_{\max}$ and the related dissipation $D_{\max}$, representing a maximum possible given the thermal structure of the atmosphere. In their study, PH also found $\eta_{\max}$. The efficiency η relates to the magnitude of kinetic energy generation and $\eta_{\max}$ to the sum of all irreversible sources of entropy. After SG, expressions of their model results, and derived quantities, are presented in Table 3. In the last two columns, values come from section 2 (s2) and PH. The agreement between items 2 and 3 seems highly satisfactory. Item 7 shows the efficiency η; this relates to $\eta_S = 2.0\%$ from section 2 and $\eta_k = 0.6\%$ from PH, who did not include any water loading in respect of η_k. Items 8 and 9 show the efficiency $\eta_{\max}$. After section 2 an efficiency of 9.7% is found by dividing the total dissipation 14.9 W m^{-2} by $F_h = 153$ W m^{-2}. This 9.7% matches closely the

Unauthenticated | Downloaded 10/23/21 01:08 AM UTC

TABLE 3. Results from and after SG. Among the main entries, all except items 8, 14, and 15 are derived from Table 1 of SG. In column s2 are values after section 2, and in column PH from PH.

Model run		S1	S2	S3	s2	PH
1. Total surface energy flux (W m^{-2})	F_h	647	416	295		
2. Energy sink in deep convective layer (W m^{-2})	αF_h	431	277	196		
3. Power output by convection (W m^{-2})	M_c ΔMSE	408	296	241		
4. Convective mass flux (kg m^{-2} s^{-1}).	M_c	0.078	0.041	0.027		
5. MSE difference: updraft − environment (J kg^{-1})	ΔMSE	5226	7214	8940		
6. Parcel theory estimate of energy (J kg^{-1})	CAPE	1143	997	998		
7. Efficiency = D_{tot}/F_h from buoyancy flux [Eq. (19) of SG]	η	4.4%	3.5%	2.7%	2.0%	0.6%
8. Efficiency = α CAPE/ΔMSE [Eq. (15) of SG]	$\eta_{\max}$	15%	9.2%	7.4%	9.7%	8.7%
9. Efficiency from thermal data [Eq. (13) of SG]	$\eta_{\max}$	13%	11%	10%	9.7%	8.7%
10. Kinetic energy of convective motions (J kg^{-1})	w_*^2	14.4	14.4	14.4		
11. Mechanical dissipation (W m^{-2})	$w_*^2 M_c$	1.1	0.6	0.4	0.75	1.0
12. Efficiency of kinetic energy generation	w_*^2/ΔMSE	0.28%	0.20%	0.16%	0.49%	0.6%
13. Area coverage from model	σ	2.1%	1.1%	0.7%		
14. Area coverage from theory [Table 2 of SG]	σ	3.4%	2.0%	1.4%		
15. Area coverage from Eq. (3.4) here	σ	2.3%	0.9%	0.5%		

value of $\eta_{\max}$ given as item 9, so the 14.9 W m^{-2} appears to be akin to $D_{\max}$ of SG. In their study, PH gave 8.7% for $\eta_{\max}$, in good agreement.

A relationship is sought between the mechanical term in Table 2 and the results of SG. Dissipation related to the kinetic energy w_*^2, reckoned as $w_*^2 M_c$, is shown as item 11. These values are quite close to the mechanical dissipation 0.75 W m^{-2} related to the efficiency η_S. An efficiency of generation of kinetic energy, w_*^2/ΔMSE, is sought in item 12. To match this the efficiency $\eta_w = 0.75/153 = 0.49\%$ is suggested. It is seen to be quite close to the values from SG. The efficiency η_k of PH, 0.6%, is appropriate here rather than with item 7, and is about the same. Nice results are obtained by expressing the kinetic energy as

$$w_*^2 \approx \eta_w \Delta\text{MSE} \tag{3.3}$$

with η_w set to 0.49%. From (3.1), (3.2), and (3.3) it follows that the fractional updraft area is given by

$$\sigma \approx \alpha F_h/[\rho \Delta\text{MSE}^{3/2} \eta_w^{1/2}]. \tag{3.4}$$

Craig (1996) found that the power-law dependencies in this equation must relate to the nondimensional quantity $F_h/(\rho\ \Delta\text{MSE}^{3/2})$. The analysis of RI leads to an equation very similar to (3.4) if their radiation time constant is eliminated in favor of convective updraft velocity by substituting their Eqs. (32) and (35) into their Eq. (37), and (3.3) above is then used for the velocity. Equation (26) of EB resembles (3.4). Klein (1997)[2] also found consistency between the work of RI and EB. Equations of RI and of EB have the same power-law dependence as (3.4), directly with Craig. Equation (29) of SG is different in that, after working with w_*^3 in respect of mechanical dissipation, the nondimensional quantity is raised to the power 2/3:

$$\sigma \approx \alpha(F_h/\rho)^{2/3}(\eta^{1/3}\Delta\text{MSE})^{-1}. \tag{3.5}$$

Values of σ obtained from the model runs and from Eqs. (3.5) and (3.4), with η taken from item 7, are included in Table 3. Equation (3.4) yields better agreement with the model than (3.5). The values of σ are larger than the value 0.5% adopted in section 2: the forcing and the precipitation rate of SG were very intense.

The scenario modeled by SG is quite similar to the winter monsoon conditions over the South China Sea examined by Warner (1981, 1982). Fractional area coverage by small cumulus updrafts at low levels modeled by SG reached 5%. Similar coverage was reached occasionally by cumulus fractus and humilis over the South China Sea (Warner 1981 Table 2). In their study, SG (their Fig. 8) showed coverage down to 2%–0.5% in the low troposphere, whereas Warner (1981) reported tenths of 1%. Model resolution must be important for cumulus congestus and cumulonimbus, so the general agreement appears to be encouraging.

5. Summary

A review of irreversible sources of entropy in a tropical oceanic system in radiative–convective equilibrium, involving both observations and results from numerical models (in particular the three-dimensional model of Tompkins and Craig 1998), has led to clarification and reconciliation of estimates from different authors. Recycling of moisture is shown to be important. After a precipitation efficiency of 36% derived from the modeling of Tompkins and Craig, it is found that evaporation of precipitation contributes about 37% of the total irreversible production of entropy. Falling precipitation contributes about 30%. Mixing of unsaturated parcels of air contributes about 15% of the total production. Evaporation from the surface accounts for 11%. The remaining 7% is accounted for by turbulent kinetic en-

[2] See also the related replies to this comment by Emanuel and Bister (1997) and Rennó (1997).

Unauthenticated | Downloaded 10/23/21 01:08 AM UTC

ergy, generation of gravity waves, and sensible heating at the surface.

A mechanical efficiency of conversion of heat supply at the surface into kinetic energy of the direct circulation, ≈2.0%, was obtained after the budget study. The leading term is due to the effect of hydrometeors. Drag of hydrometeors was split into two components based on relative contributions of form drag plus water loading (50%) and frictional drag (50%); only the former contributes to the direct circulation. The contribution of turbulent kinetic energy was found to be small. The mechanical efficiency η_S was found to be relatively insensitive to the area-wide mean precipitation rate.

Comparison of the budget studies with studies of CAPE by Roff and Yano (2002) suggest that a singularity is reached when there is sufficient APE to drive a direct local convective circulation. Consistency of results from the budget study was found also with modeling and theoretical work by Shutts and Gray (1999).

Acknowledgments. I thank Brian Mapes and members of the Atmospheric Technology Division of the National Center for Atmospheric Research for providing the sounding data used in the course of my studies, and many people, including Peter Bannon, Gary Barnes, David Bleasdale, George Craig, Kerry Emanuel, Richard Goody, Donald Johnson, T. N. Krishnamurti, Brian Mapes, Olivier Pauluis, David Randall, Nilton Rennó, and anonymous referees for suggestions, encouragement, and other help. Melanie Odell and her staff at Grayswood Computer Services have always been very kind.

REFERENCES

Austin, P. M., and S. G. Geotis, 1979: Raindrop sizes and related parameters for GATE. *J. Appl. Meteor.,* **18,** 569–575.

Baker, M. B., R. E. Breidenthal, T. W. Choularton, and J. Latham, 1984: The effects of turbulent mixing in clouds. *J. Atmos. Sci.,* **41,** 299–304.

Bannon, P. R., 2002: Theoretical foundations for models of moist convection. *J. Atmos. Sci.,* **59,** 1967–1982.

Braham, R. R., Jr., and P. Spyers-Duran, 1967: Survival of cirrus crystals in clear air. *J. Appl. Meteor.,* **6,** 1053–1061.

Carpenter, R. L., Jr., K. K. Droegemeier, and A. M. Blyth, 1998: Entrainment and detrainment in numerically simulated cumulus congestus clouds. Part I: General results. *J. Atmos. Sci.,* **55,** 3417–3432.

Comstock, J. M., T. P. Ackerman, and G. G. Mace, 2002: Ground-based lidar and radar remote sensing of tropical cirrus clouds at Nauru Island: Cloud statistics and radiative impacts. *J. Geophys. Res.,* **107**, 4714, doi:10.1029/2002JD002203.

Craig, G. C., 1996: Dimensional analysis of a convecting atmosphere in equilibrium with external forcing. *Quart. J. Roy. Meteor. Soc.,* **122,** 1963–1967.

Emanuel, K. A., and M. Bister, 1996: Moist convective velocity and buoyancy scales. *J. Atmos. Sci.,* **53,** 3276–3285.

——, and ——, 1997: Reply. *J. Atmos. Sci.,* **54,** 2778–2779.

Garstang, M., and D. R. Fitzjarrald, 1999: *Observations of Surface to Atmosphere Interactions in the Tropics.* Oxford University Press, 405 pp.

Geldmeier, M. F., and G. M. Barnes, 1997: The "footprint" under a decaying tropical mesoscale convective system. *Mon. Wea. Rev.,* **125,** 2879–2895.

Gettelman, A., M. L. Salby, and F. Sassi, 2002: Distribution and influence of convection in the tropical tropopause region. *J. Geophys. Res.,* **107**, 4080, doi:10.1029/2001JD001048.

Goody, R., 2000: Sources and sinks of climate entropy. *Quart. J. Roy. Meteor. Soc.,* **126,** 1953–1970.

——, 2003: On the mechanical efficiency of deep, tropical convection. *J. Atmos. Sci.,* **60,** 2827–2832.

Gray, W. M., and R. W. Jacobson Jr., 1977: Diurnal variation of deep cumulus convection. *Mon. Wea. Rev.,* **105,** 1171–1188.

Heymsfield, A. J., and L. J. Donner, 1990: A scheme for parameterizing ice-cloud water content in general circulation models. *J. Atmos. Sci.,* **47,** 1865–1877.

Hildebrand, P. H., 1998: Shear-parallel moist convection over the tropical ocean: A case study from 18 February 1993 TOGA COARE. *Mon. Wea. Rev.,* **126,** 1952–1976.

Houze, R. A., Jr., and A. K. Betts, 1981: Convection in GATE. *Rev. Geophys. Space Phys.,* **19,** 541–576.

Huffman, G. J., and Coauthors, 1997: The Global Precipitation Climatology Project (GPCP) combined precipitation dataset. *Bull. Amer. Meteor. Soc.,* **78,** 5–20.

Iwasa, Y., Y. Abe, and H. Tanaka, 2002: Structure of the atmosphere in radiative–convective equilibrium. *J. Atmos. Sci.,* **59,** 2197–2226.

Johnson, R. H., and R. A. Houze Jr., 1987: Precipitating cloud systems of the Asian monsoon. *Monsoon Meteorology*, C.-P. Chang and T. N. Krishnamurti, Eds., Oxford University Press, 298–353.

Jorgensen, D. P., and P. T. Willis, 1982: A *Z–R* relationship for hurricanes. *J. Appl. Meteor.,* **21,** 356–366.

——, M. A. LeMone, and S. B. Trier, 1997: Structure and evolution of the 22 February 1993 TOGA COARE squall line: Aircraft observations of precipitation, circulation, and surface energy fluxes. *J. Atmos. Sci.,* **54,** 1961–1985.

Kershaw, R., 1995: Parametrization of momentum transport by convectively generated gravity waves. *Quart. J. Roy. Meteor. Soc.,* **121,** 1023–1040.

Klein, S. A., 1997: Comments on "Moist convective velocity and buoyancy scales." *J. Atmos. Sci.,* **54,** 2775–2777.

Kley, D., and Coauthors, 1997: Tropospheric water-vapour and ozone cross-sections in a zonal plane over the central equatorial Pacific Ocean. *Quart. J. Roy. Meteor. Soc.,* **123,** 2009–2040.

Lac, C., J.-P. Lafore, and J.-L. Redelsperger, 2002: Role of gravity waves in triggering deep convection during TOGA COARE. *J. Atmos. Sci.,* **59,** 1293–1316.

Lane, T. P., M. J. Reeder, and T. L. Clark, 2001: Numerical modeling of gravity wave generation by deep tropical convection. *J. Atmos. Sci.,* **58,** 1249–1274.

Le Clair, B. P., A. E. Hamielec, and H. R. Pruppacher, 1970: A numerical study of the drag on a sphere at low and intermediate Reynolds numbers. *J. Atmos. Sci.,* **27,** 308–315.

Lucas, C., E. J. Zipser, and M. A. LeMone, 1994: Vertical velocity in oceanic convection off tropical Australia. *J. Atmos. Sci.,* **51,** 3183–3193.

Ludlam, F. H., 1980: *Clouds and Storms.* The Pennsylvania State University Press, 405 pp.

Pauluis, O., and I. M. Held, 2002: Entropy budget of an atmosphere in radiative–convective equilibrium. Part I: Maximum work and frictional dissipation. *J. Atmos. Sci.,* **59,** 125–139.

——, V. Balaji, and I. M. Held, 2000: Frictional dissipation in a precipitating atmosphere. *J. Atmos. Sci.,* **57,** 989–994.

Peixoto, J. P., and A. H. Oort, 1992: *Physics of Climate*. American Institute of Physics, 520 pp.

Pfister, L., S. Scott, M. Loewenstein, S. Bowen, and M. Legg, 1993: Mesoscale disturbances in the tropical stratosphere excited by convection: Observations and effects on the stratospheric momentum budget. *J. Atmos. Sci.,* **50,** 1058–1075.

Pond, S., G. T. Phelps, J. E. Paquin, G. McBean, and R. W.

Unauthenticated | Downloaded 10/23/21 01:08 AM UTC

Stewart, 1971: Measurements of the turbulent fluxes of momentum, moisture, and sensible heat over the ocean. *J. Atmos. Sci.,* **28,** 901–917.

Pruppacher, H. R., and J. D. Klett, 1997: *Microphysics of Clouds and Precipitation*. Kluwer, 954 pp.

Rennó, 1997: Reply: Remarks on natural convection as a heat engine. *J. Atmos. Sci.,* **54,** 2780–2782.

——, 2001: Comments on "Frictional dissipation in a precipitating atmosphere." *J. Atmos. Sci.,* **58,** 1173–1177.

——, and A. P. Ingersoll, 1996: Natural convection as a heat engine: A theory for CAPE. *J. Atmos. Sci.,* **53,** 572–585.

Riehl, H., and J. M. Simpson, 1979: The heat balance of the equatorial trough zone, revisited. *Contrib. Atmos. Phys.,* **52,** 287–305.

Roff, G. L., and J.-I. Yano, 2002: Tropical convective variability in the CAPE phase space. *Quart. J. Roy. Meteor. Soc.,* **128,** 2317–2333.

Roux, F., 1998: The oceanic mesoscale convective system observed with airborne Doppler radars on 9 February 1993 during TOGA-COARE: Structure, evolution and budgets. *Quart. J. Roy. Meteor. Soc.,* **124,** 585–614.

Scorer, R. S., 1986: *Cloud Investigation by Satellite*. Ellis Horwood, 317 pp.

Sherwood, S. C., 1996: Maintenance of the free-tropospheric tropical water vapor distribution. Part II: Simulation by large-scale advection. *J. Climate,* **9,** 2919–2934.

Shie, C.-L., W.-K. Tao, J. Simpson, and C.-H. Sui, 2003: Quasi-equilibrium states in the Tropics simulated by a cloud-resolving model. Part I: Specific features and budget analysis. *J. Climate,* **16,** 817–833.

Shutts, G. J., and M. E. B. Gray, 1999: Numerical simulations of convective equilibrium under prescribed forcing. *Quart. J. Roy. Meteor. Soc.,* **125,** 2767–2787.

Stephens, G. L., and D. M. O'Brien, 1993: Entropy and climate. I: ERBE observations of the entropy production of the earth. *Quart. J. Roy. Meteor. Soc.,* **119,** 121–152.

Sui, C. H., K. M. Lau, W. K. Tao, and J. Simpson, 1994: The tropical water and energy cycles in a cumulus ensemble model. Part I: Equilibrium climate. *J. Atmos. Sci.,* **51,** 711–728.

Tompkins, A. M., and G. C. Craig, 1998: Radiative–convective equilibrium in a three-dimensional cloud-ensemble model. *Quart. J. Roy. Meteor. Soc.,* **124,** 2073–2097.

Warner, C., 1981: Photogrammetry from aircraft side camera movies: Winter MONEX. *J. Appl. Meteor.,* **20,** 1516–1526.

——, 1982: Mesoscale features and cloud organization on 10–12 December 1978 over the South China Sea. *J. Atmos. Sci.,* **39,** 1619–1641.

——, 1984a: Core structure of a Bay of Bengal monsoon depression. *Mon. Wea. Rev.,* **112,** 137–152.

——, 1984b: Stereo-pair photographs of monsoon clouds. *Bull. Amer. Meteor. Soc.,* **65,** 344–347.

——, 2003: Stereo-pair photographs of clouds. *Weather,* **58,** 84–89.

——, and R. H. Grumm, 1984: Cloud distributions in a Bay of Bengal monsoon depression. *Mon. Wea. Rev.,* **112,** 153–172.

——, and D. P. McNamara, 1984: Aircraft measurements of convective draft cores in MONEX. *J. Atmos. Sci.,* **41,** 430–438.

——, J. H. Renick, M. W. Balshaw, and R. H. Douglas, 1973: Stereo photogrammetry of cumulonimbus clouds. *Quart. J. Roy. Meteor. Soc.,* **99,** 105–115.

——, J. Simpson, G. Van Helvoirt, D. W. Martin, D. Suchman, and G. L. Austin, 1980: Deep convection on day 261 of GATE. *Mon. Wea. Rev.,* **108,** 169–194.

Zipser, E. J., and M. A. LeMone, 1980: Cumulonimbus vertical velocity events in GATE. Part II: Synthesis and model core structure. *J. Atmos. Sci.,* **37,** 2458–2469.

Unauthenticated | Downloaded 10/23/21 01:08 AM UTC